BBA - Bioenergetics 1860 (2019) 148081

Contents lists available at ScienceDirect

BBA - Bioenergetics

journal homepage: www.elsevier.com/locate/bbabio

Regulation of photosynthetic cyclic electron flow pathways by adenylate status in higher plant chloroplasts

Nicholas Fisher[a], Terry M. Bricker[c], David M. Kramer[a,b,*]

[a] MSU-DOE Plant Research Laboratory, Michigan State University, East Lansing, MI 48824, United States of America
[b] Biochemistry and Molecular Biology, Michigan State University, East Lansing, MI 48824, United States of America
[c] Department of Biological Sciences, Biochemistry and Molecular Biology Section, Louisiana State University, Baton Rouge, LA 70803, United States of America

ARTICLE INFO

Keywords:
Photosynthesis
Cyclic electron flow
Regulation
Enzymology

ABSTRACT

Cylic electron flow (CEF) around Photosystem I in photosynthetic eukaryotes is likely to be necessary to augment ATP production, rapidly- and precisely balancing the plastid ATP/NADPH energy budget to meet the demands of downstream metabolism. Many regulatory aspects of this process are unclear. Here we demonstrate that the higher plant plastid NADH/Fd:plastoquinone reductase (NDH) and proposed PGR5/PGRL1 ferredoxin:plastoquinone reductase (FQR) pathways of CEF are strongly, rapidly and reversibly inhibited *in vitro* by ATP with K_i values of 670 μM and 240 μM respectively, within the range of physiological changes in ATP concentrations. Control experiments ruled out effects on secondary reactions, *e.g.* FNR- and cytochrome b_6f activity, nonphotochemical quenching of chlorophyll fluorescence *etc.*, supporting the view that ATP is an inhibitor of CEF and its associated *pmf* generation and subsequent ATP production. The effects are specific to ATP, with the ATP analog AMP-PNP showing little inhibitory effect, and ADP inhibiting only at higher concentrations. For the FQR pathway, inhibition was found to be classically competitive with Fd, and the NDH pathway showing partial competition with Fd. We propose a straightforward model for regulation of CEF in plants in which CEF is activated under conditions when stromal ATP low, but is downregulated as ATP levels build up, allowing for effective ATP homeostasis. The differences in K_i values suggest a two-tiered regulatory system, where the highly efficient proton pumping NDH is activated with moderate decreases in ATP, with the less energetically-efficient FQR pathway being activated under more severe ATP depletion.

1. Introduction

In the linear electron flow (LEF) pathway of oxygenic photosynthesis, energy from light is stored by extracting electrons from water and transferring them through a series of membrane-bound and soluble redox carriers to reduce $NADP^+$. During this process a chemiosmotic proton electrochemical gradient (proton motive force, *pmf*) is established across the thylakoid membrane (at a ratio of $6H^+/2e^-$), which is harnessed by the plastid (CF_oF_1)-ATP synthase to storing more energy in the synthesis of ATP from ADP and inorganic phosphate [1]. The osmotic component of *pmf*, ΔpH, also plays a central role in the regulation of the light reactions of photosynthesis, by acidifying the thylakoid lumen, which triggers the activation of 'energy dependent' (q_E) component of nonphotochemical quenching (NPQ), which, through the participation of photosystem PsbS and the xanthophyll cycle, dissipates excess energy from light (which can lead to photodamage due to oxygen radical production) as heat [2,3]. Photosynthetic control by the slowing of plastoquinol (PQH_2) oxidation by the cytochrome b_6f complex as lumenal pH decreases, is also critical for preventing the accumulation of electrons on Photosystem I (PSI) centers, which can lead to photodamage [1,4,5].

The *pmf*-regulatory system also responds to changes in the physiological and metabolic states of the cell. The activity of the ATP synthase can be down-regulated to retard proton efflux, increasing *pmf* and down-regulation of the light reactions [1]. In addition, the regulatory impact of *pmf* can be altered by adjusting fluxes of counterions across the thylakoid membrane through the action of various ion transporters or permeable buffers [6]. Furthermore, the responses of q_E to lumen pH may be modulated by altering the expression of q_E-related components [1,7].

Another important constraint on photosynthesis is the need to balance the "plastid energy budget", the ratios of ATP/NADPH produced to precisely match their consumption by downstream biochemistry, thus avoiding metabolic congestion. The ATP/NADPH production ratio

* Corresponding author at: MSU-DOE Plant Research Laboratory, 612 Wilson Rd., Michigan State University, East Lansing, MI 48824, United States of America.
E-mail address: kramerd8@msu.edu (D.M. Kramer).

https://doi.org/10.1016/j.bbabio.2019.148081
Received 28 May 2019; Received in revised form 1 September 2019; Accepted 8 September 2019
Available online 11 September 2019
0005-2728/

for LEF is determined by the tight coupling of the proton- and electron transferring reactions of LEF, and the ratio of protons translocated through the ATP synthase for each ATP synthesized (H^+/ATP), which is governed by the subunit stoichiometry of the proton-translocating c-ring stoichiometry. Assuming that $3H^+$ are translocated into the lumen for each electron transferred from water to Fd, and a H^+/ATP ratio of 4.67 (based on a c-subunit stoichiometry of 14), results in an ATP/NADPH production ratio of about 1.3:1. This falls short of the 1.5:1 requirement of the carbon-fixing reactions of the Calvin-Benson-Bassham (CBB) cycle, as well as changes in the engagement of other assimilatory and biosynthetic processes, such as nitrite reduction, ion/metabolite transport and protein/DNA synthesis [1,4].

The most cited process proposed to provide fine balancing of ATP/NADPH in the chloroplast is cyclic electron flow (CEF) around PSI (see reviews in [8–10]). In CEF, electrons from photoexcited PSI are recycled back into the thylakoid plastoquinone (PQ) pool *via* a PQ reductase (PQR), resulting in proton flux through the ATP synthase, but no net production of NADPH. The buildup of *pmf* can also activate photoprotective mechanisms [4,9]. At least three PQR reductases have been proposed to function in higher plant CEF (see review in ([10]); i) the protonmotive Fd/NADPH dehydrogenase complex (NDH), an analog of respiratory Complex I; ii) the antimycin A-sensitive Fd:PQ reductase, which is proposed to be associated with the PGR5 and/or PGRL1 proteins; and iii) direct reduction of heme b_H (or heme c_i) within the cytochrome b_6f complex by Fd with associated PQ reduction *via* the Q_i site of this complex. These pathways may operate in parallel or in an organism-specific manner, NDH-CEF is likely to be the most energy efficient, with a proposed $H^+/2e^-$ ratio of 8, with the others (through associated b_6f Q-cycle activity) most likely yielding 4 [9–11].

CEF appears to be only incrementally activated under non-stressed, steady-state conditions in C3 plants, when LEF nearly meets the ATP required for chloroplast metabolism, but up-regulated when high ATP demand is expected, *e.g.* under environmental stress, during induction of photosynthesis in dark-adapted plants [12], or in mutants with modified ATP/NADPH demands [13]. CEF is thought to play a larger role in supplementing the ATP needed to drive the CO_2 concentrating mechanisms in green algae or in C4 photosynthesis [14,15]. Note that *Amaranthus hybridus*, the subject of the current study, uses the NAD-malic enzyme C4 pathway, with enriched NDH content in mesophyll chloroplasts *versus* the bundle sheath [15]. CEF may also play a regulatory role *via* its acidification of the thylakoid lumen, but it is important to note that increasing CEF will also increase the output of ATP relative to NADPH, and the resulting energy imbalances may limit the extent to which CEF can contribute to activation of NPQ [1,16]. It is important to note that other processes, such as the control of proton efflux by modulation of the ATP synthase, and partitioning of *pmf* into ΔpH can account for modulation of q_E responses (see discussion in [17]).

Given that different CEF pathways may operate in different organisms under different conditions, we expect there to be a range of regulatory systems that fine tune their activities. However, if the major role of CEF is to balance ATP/NADPH output, it seems likely that its regulation will, either directly or indirectly, respond to the adenylate or redox state of the chloroplasts. Within this context, there are many possible regulatory components that can sense these factors, and these may operate simultaneously to fine tune the engagement of CEF. Contrary to earlier proposals, state transitions (the phosphorylation-associated migration of LHCII antenna between photosystems I- and II) do not appear to regulate CEF in plants and algae [18–20]. Based on observations of CEF activation during induction of photosynthesis in spinach and *Arabidopsis thaliana* leaves under moderate osmotic stress, Joliot proposed that ATP levels may regulate CEF through the b_6f complex:PSI supercomplexes, which were proposed to dissociate as the stromal ATP concentration increases, favoring LEF [12]. More recently, Ca^{2+} has been proposed to regulate CEF *via* the chloroplast-localized calcium sensor protein (CAS) [21], which also modulates stomatal conductance in *A. thaliana*, and controls expression of LHCSR3 in *Chlamydomonas reinhardtii*, a component of the q_E pathway in this organism [22,23]. Furthermore, CAS has been proposed to interact with the PGRL1 protein in the *C. reinhardtii*, forming a supercomplex containing PSI, PGRL1, ferredoxin:$NADP^+$ oxidoreductase (FNR) and b_6f, although the importance of this complex in CEF is still being debated [21]. A novel Ca^{2+}-binding chloroplast-localized thioredoxin, calredoxin, has been characterized in *C. reinhardtii*, with its activity associated with stress acclimation and increased activation of CEF, linking CEF regulation to the complex network of thiol-regulated processes within the chloroplast [24,25]. Relatedly, we have shown that hydrogen peroxide induces NDH-CEF in *A. thaliana*, either directly, or by redox modulation of key enzymes, possibly linking changes in the redox status of the stroma with the regulation of CEF in higher plants [26]. We also reported that the FQR activity requires reduction of thiols, suggesting that redox status may be involved in CEF regulation [27]. However, it has remained unclear how the NDH-CEF and FQR-CEF are regulated in responses to rapid changes in the relative demands for ATP and NADPH imposed by environmental conditions, including rapid fluctuations in light intensities.

Recently, we demonstrated that NDH in vascular plants can catalyze high-efficiency CEF by acting as a proton pump [11]. During this work, we explored the effects of thylakoid *pmf* on NDH activity. One approach was to produce *pmf* in thylakoids by running the chloroplast ATP synthase in "reverse," hydrolyzing ATP to translocate protons into the lumen. Surprisingly addition of ATP to uncoupled thylakoids led to strong inhibition of NDH, whereas light-induced *pmf* of similar amplitude did not, leading us to hypothesize that ATP acts as an inhibitor of NDH. In this work, we present evidence that ATP inhibition constitutes regulatory mechanisms for both NDH- and FQR-CEF that responds rapidly to changes in stromal ATP, to maintain energy homeostasis.

2. Materials and methods

2.1. Reagents and plant material

Reagents were purchased from Sigma-Aldrich unless otherwise noted. Ferredoxin was prepared from market-bought spinach as described in [28].

A. hybridus (cv. 'Opopeo') seeds were originally obtained from Swallowtail Garden Seeds (Santa Rosa, CA), with the plants grown in vermiculite under a 16 h:8 h (light:dark) photoperiod (white fluorescent illumination at 100 μmol of photons $m^{-2} s^{-1}$) at 30 °C. *A. thaliana* Col-0 and STN7 (SALK 073254) were grown in peat-based potting media using a 16 h:8 h (light:dark) photoperiod (white fluorescent illumination at 100 μmol of photons $m^{-2} s^{-1}$) at 21 °C. Spinach was purchased from a local market, with chloroplasts prepared- and used on the day of purchase.

2.2. Chloroplast preparation and chlorophyll quantification

Chloroplasts from spinach, *A. hybridus* and *A. thaliana* were prepared on ice as described in [28], using 21–28 day-old *A. hybridus* and *A. thaliana* plants. DTT was reduced with sodium borohydride prior to inclusion in the leaf grinding buffer at a final concentration of 2 mM as described in [27]. Crude chloroplast preparations were resuspended to a chlorophyll concentration of 2–4 mg/ml in grinding medium (0.33 M sorbitol, 2 mM EDTA, 5 mM $MgCl_2$, 2 mM (reduced) DTT, 5 mM ascorbate, 0.1% (w/v) BSA, 50 mM HEPES, pH 7.6). Chlorophyll was quantitated using the method as described in [27].

2.3. Post illumination (chlorophyll) fluorescence rise measurements

All *in vitro* assays described in this study were performed at 21 °C unless stated otherwise.

The post illumination (chlorophyll) fluorescence rise was measured

in broken chloroplast preparations from spinach, *A. hybridus* and *A. thaliana* as described in [11]. Chloroplasts were osmotically shocked on ice for 30s *in situ*, with the samples consisting of 50 μg Chl/ml in 10 mM HEPES (pH 7.6), supplemented with 5 mM $MgCl_2$, 10 mM KCl, 1 μM Fd, 100 μM NADPH, 10 μM nigericin and 10 μM valinomycin. Antimycin A, when used, was present at 10 μM. Chlorophyll fluorescence was measured using a laboratory-constructed spectrofluorimeter [29], with a cyan (505 nm) measuring pulse at an intensity of 0.5 μmol of photons $m^{-2} s^{-1}$.

For the PIFR assays discussed here, samples were maintained and manipulated under dim green illumination (~0.1 μmol photons $m^{-2} s^{-1}$) prior to the start of measurement, the PQ pool was pre-reduced nonphotochemically by the presence of exogenous NADPH and Fd, and so fluorescence data were not normalised to F_o. After initial dark adaptation, samples were illuminated with a pulse of saturating red light (1 s, 620 nm, 5000 μmol photons $m^{-2} s^{-1}$), allowing determination of F_v/F_m, followed by 60 s of actinic illumination (620 nm, 250 μmol photons $m^{-2} s^{-1}$), during which both species reached the Fs′ steady state fluorescence level (Fs′). The actinic light was then switched off, during which time the fluorescence yield decreased (F_s*), and was then further decreased by the application of far red light (720 nm, 50 μmol photons $m^{-2} s^{-1}$) for 15 s, preferentially driving PSI photochemistry to oxidize the PQ pool, at which point the fluorescence yield with oxidized Q_A (F_o*) was recorded. When the far red light was switched off, the fluorescence rose again due to the reduction of PQ by PQ reductases, reaching a steady state level (F_{p1}). The pattern was repeated upon additional applications of far red illumination (reaching F_{o2}*) and darkness (F_{p2}). Finally, a second saturating flash was applied at the end of the experiment, and the maximal fluorescence at the end (F_{m2}). F_{m1} and F_{m2} were consistently within a few percent of each other, indicating that changes in fluorescence yield caused by state transitions, NPQ or photodamage, were minimal. The initial rate of the PIFR was obtained by linear regression (typically for a 10s range) on Fo* normalised fluorescence data using Kaleidagraph (Synergy Software, PA).

2.4. FNR (NADPH/Fd:cytochrome c reductase) activity assay

FNR-mediated NADPH/Fd:cytochrome *c* reductase activity was measured spectrophotometrically at 550- *minus* 542 nm in a laboratory constructed spectrophotometer as described in [28]. Spinach FNR was purchased from Sigma-Aldrich and used without further purification. The reaction medium consisted of 10 mM HEPES (pH 7.6), 5 mM $MgCl_2$, 1 μM spinach Fd, 20 μM equine cytochrome *c* and approximately 1 μg of spinach FNR. The reaction was initiated by the addition of 100 μM NADPH.

2.5. P700 redox spectrophotometry

P700 redox changes in osmotically ruptured spinach and *A. hybridus* chloroplasts (50 μg Chl/ml) were monitored in a laboratory-constructed spectrophotometer [29] utilizing a pulsed 720 nm LED filtered through a 700 nm bandpass filter (10 nm bandwidth, Edmund Optics) as the measuring beam source. Actinic light (620 nm) was provided at 250 μmol photons $m^{-2} s^{-1}$. The assay medium consisted of 10 mM HEPES (pH 7.6), 5 mM $MgCl_2$, 10 mM KCl, 1 μM spinach Fd, 100 μM NADPH, 1 mM hydroxylamine, 10 μM DCMU, 10 μM nigericin, and 10 μM valinomycin. Antimycin A, when used, was present at 10 μM.

2.6. LEF-dependent ferricyanide photoreduction

Ferricyanide photoreduction was measured in a laboratory-constructed spectrophotometer utilizing a pulsed (10 Hz) white LED (0.1 μmol photons $m^{-2} s^{-1}$, 420 nm bandpass-filtered, 10 nm bandwidth, Edmund Optics), with a BG18-filtered detector. Actinic light (620 nm) was provided at 250 μmol photons $m^{-2} s^{-1}$. Broken chloroplasts were resuspended to 40 μg Chl/ml in assay medium consisting of 10 mM HEPES (pH 7.6), 5 mM $MgCl_2$, 10 mM KCl, 10 μM nigericin, 10 μM valinomycin and 200 μM potassium ferricyanide.

2.7. Antenna cross-sectional area

Antenna cross-sectional area in spinach and *A. hybridus* broken chloroplast preparations was measured in the spectrofluorimeter described for the PIFR assay above. Chloroplasts were resuspended to 50 μg Chl/ml in 10 mM HEPES (pH 7.6), 5 mM $MgCl_2$, 10 mM KCl, 1 μM Fd, 100 μM NADPH, 10 μM nigericin, 10 μM valinomycin. Antimycin A was included at 10 μM for the *A. hybridus* experiments. The (cyan) measuring pulse frequency was 10 Hz (0.5 μmol photons $m^{-2} s^{-1}$), with two weakly actinic flashes (600 ms duration, 620 nm, 100 μmol photons $m^{-2} s^{-1}$) separated by an interval of 3 min.

2.8. ODE simulation of stromal adenylate equilibria

Steady-state concentrations of AMP, ADP and ATP as a function of phosphorylation potential (ΔG_P) were modeled using a simple 1st order ordinary differential equation solver provided online by Prof. Robert Hanson (St Olaf College, MN) at https://www.stolaf.edu/depts/chemistry/courses/toolkits/126/js/kinetics/.The stromal adenylate pool was set to physiologically relevant composition initial concentrations of AMP, ADP, ATP and Pi (0.6-, 2-, 0- and 4 mM respectively) and allowed to equilibrate, *via* adenylate kinase, as in [30,31] and ΔG^o for ATP hydrolysis assumed to be $-30.5\ kJ\ mol^{-1}$ [32]. Kinetic simulations were run for 1000 (arbitrary) time points, by which point the concentrations of all components had reached a steady state.

3. Results

3.1. Evidence for inhibition of CEF by ATP

The post illumination fluorescence rise (PIFR) signal observed as a rise in the (chlorophyll) fluorescence quantum yield following light-dark transition, and reflects the accumulation (and equilibration) of electrons on Q_A within PSII as the PQ pool becomes progressively reduced in the dark by the activity of PQ reductases in the thylakoid (Fig. 1A) [11,33–35]. The PIFR signal *in vivo* is typically associated with the activity of NDH, and has been used in high throughput screening to isolate mutants defective in the synthesis and activity of the NDH complex [34,36]. *In vitro*, the assay has been used to estimate the rates of both NDH and FQR-CEF, though certain controls are needed to eliminate alternative interpretations of the signal [11,28,37]. Far-red illumination was periodically applied during the dark phase of the PIFR experiment to preferentially drive PSI photochemistry, oxidizing the PQ pool and hence favorably poising the system for repeated measurement of the PIFR during the course of a single assay. Without further additions, a sequence of more than five consistently reproducible PIFR signals can be obtained in a single run [11].

Fig. 1A, shows complete traces for typical *in vitro* PIFR experiments, without addition of inhibitors for spinach and *A. hybridus* broken chloroplast preparations. While the traces for the two species were qualitatively similar, PIFR was substantially faster in *A. hybridus*, likely reflecting the higher capacity for CEF in this species. The *in vitro* PIFR signals require a reductant (NADPH or NADH) and (endogenous) FNR activity, to generate reduced Fd, which acts as the electron donor substrate for NDH and FQR [11,37]. Note that all PIFR experiments described here were performed in the presence of uncouplers (10 μM nigericin, 10 μM valinomycin, 10 mM KCl) to eliminate any thermodynamic backpressure on NDH activity from CEF-generated *pmf*. In our experiments on both spinach and *A. hybridus* thylakoid preparations, no PIFR was observed in the absence of exogenous NADPH and/or Fd, demonstrating that the rise was not an artefact due to measuring beam activity, consistent with previous reports [11]. The kinetics and amplitude of the PIFR saturated at 100 μM NADPH in both spinach and *A.*

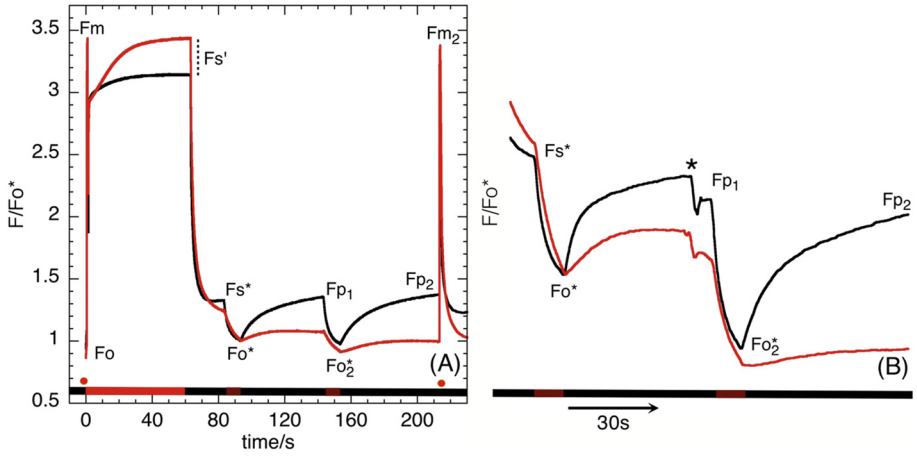

Fig. 1. (A). Post illumination fluorescence rise (PIFR) signals in *A. hybridus* (black) and spinach (red) broken chloroplast preparations antimycin A-sensitivity of the PIFR in *A. hybridus* (black) and spinach (red) thylakoids. Chloroplasts were osmotically shocked *in situ*, with the samples consisting of 50 μg Chl/ml in 10 mM HEPES (pH 7.6), supplemented with 5 mM $MgCl_2$, 10 mM KCl, 1 μM Fd, 100 μM NADPH, 10 μM nigericin and 10 μM valinomycin. The black bar along the abscissa indicated periods of darkness (black), illumination with red light (red), and illumination with far-red (maroon). Details of experiments are presented in the Materials and methods. (B) As in panel A, but with addition of 10 μM antimycin A at the point marked with an asterisk.

hybridus thylakoids, with apparent Michaelis constants (K_m) of 2.1 ± 0.6 μM and 1.3 ± 0.4 μM for (spinach) Fd in *A. hybridus* and spinach respectively (SI Fig. S1). Kinetic data were obtained from linear fits to the initial rate of the PIFR. Absolute values for V_m (and k_{cat}) cannot be ascertained from these fluorescence data, however, the relative CEF activity observed is in broad agreement with the magnitudes of CEF reported by *pmf*-dependent ACMA quenching in DCMU-inhibited spinach and *A. hybridus* thylakoid preparations [27].

It is important to note that the PIFR kinetics are complex largely due to the fact that in this assay (PSII-associated) Q_A^- is employed as a reporter for the (bulk) PQ redox state [11], and the Q_A/Q_A^- redox couple is more reducing than that of pool-localized PQ/PQH_2. Hence a kinetic 'lag' will be observed in Q_A^- accumulation until an inflection point when the PQ pool is partially reduced. However, this inflection point should be similar for all the conditions used here and thus the time required for fluorescence to increase to a particular level should be a reasonable (semiqualitative) indicator of the PQ reduction rate.

The PIFR signals were largely insensitive to antimycin A (AA) in *A. hybridus*, as indicated by the similar PIFR kinetics prior to and following addition of AA (Fig. 1B, black trace), indicating that NDH activity is the predominant CEF pathway in this genus [11,15]. By contrast, PIFR in spinach and *A. thaliana* (Fig. 1B, red trace) was inhibited AA, implying the FQR-dependent CEF pathway predominates in these species, consistent with previous reports [11,37]. The contrast between these two species and the effects of AA allowed us to study the enzymology of the two CEF pathways, and in the following we probed the NDH pathway in *A. hybridus* in the presence of antimycin A to abolish FQR activity, and the FQR pathway in spinach, checking to be sure that the majority of signal was sensitive to antimycin A.

Fig. 2 shows that PIFR signals associated predominantly with both NDH (*A. hybridus* in the presence of antimycin A, Fig. 2A) and FQR (AA-sensitive signal in spinach, Fig. 2B) were inhibited by ATP at physiologically relevant (1 mM) concentrations. Typical variability in the NDH- and FQR PIFR response to ATP is presented in Fig. S2 (SI). ADP was approximately a two- to threefold-fold weaker inhibitor than ATP at this concentration. The FQR pathway was more strongly inhibited by adenylates than the NDH pathway (Fig. 2B). AMP was a weak inhibitor of the PIFR in both spinach and *A. hybridus,* with an IC50 value of approximately 3 mM. We also investigated the sensitivity of the PIFR to the non-hydrolyzable ATP analogs adenosine 5′-(3-thiotriphosphate) (ATP-γ-S) and adenosine 5′-(β,γ-imido)triphosphate (AMP-PNP). The sensitivity of the PIFR to ATP-γ-S in spinach and *A. hybridus* broken chloroplast preparations was similar to that shown for ATP, with IC50 values of 1.1- and 0.5 mM respectively. In contrast, the PIFR in these species was insensitive to AMP-PNP (SI, Fig. S3) which suggests that the inhibition has strict steric requirements that are impacted by the bond between the adenylate β- and γ phosphates, and makes it unlikely that non-specific ionic strength effects were the origin of the ATP-dependent fluorescence quenching reported here (see discussion in [38]).

Because these samples were uncoupled we can exclude the possibility that ATP inhibition of PIFR was caused by *pmf* (*i.e.* thermodynamic backpressure) resulting from hydrolysis of ATP by the thylakoid ATP synthase. As the *in vitro* PIFR may be affected by other processes, including direct reduction of Q_A through stromal donors [28] or ATP-induced chlorophyll fluorescence quenching *in vitro* [39,40], we also examined the effect of ATP on a variety of PIFR-associated processes within our spinach- and *A. hybridus* broken chloroplast preparations, as discussed below.

Changes in antenna cross-sectional area due to the presence of exogenous adenylates might be expected to affect the kinetics and

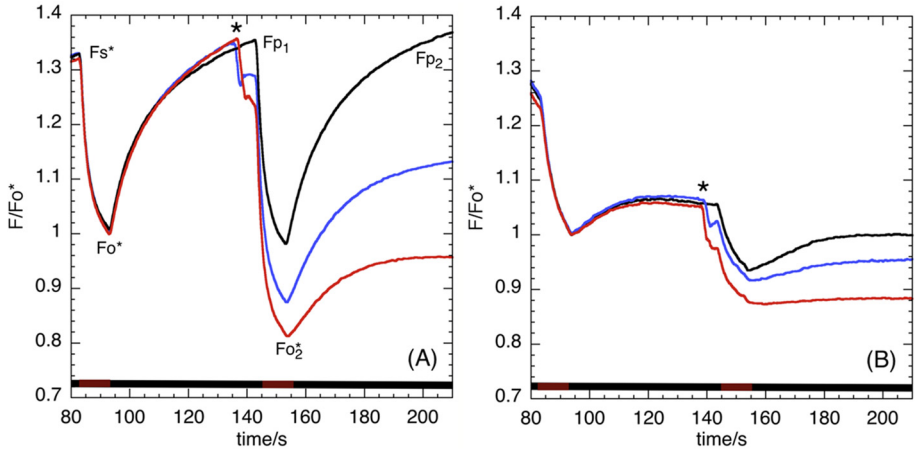

Fig. 2. The effects of adenylates on NDH and FQR activity, measured using the PIFR signal. Panels A and B, effects of ATP and ADP on PIFR signals in uncoupled thylakoid preparations from *A. hybridus* (panel A) and spinach (panel B). Experimental conditions as Fig. 1 except that 1.0 mM ATP (red) or 1.0 mM ADP (blue) were added as indicated (*) and the *A. hybridus* sample also contained 10 μM antimycin A to inhibit FQR. Control data (no adenylate additions) are presented in black. Shown are representative traces from 3 independent samples, all of which showed very similar responses. For details of the fluorescence parameters labelled in panel (A), refer to Fig. 1A or the main body of the text.

amplitude of the PIFR signal. We tested for such effects by measuring the kinetics of chlorophyll fluorescence rise induced by a weak actinic pulse (620 nm, 100 µmol photons $m^{-2} s^{-1}$) in uncoupled spinach- and *A. hybridus* thylakoid preparations in the presence of 1 µM Fd and 100 µM NADPH (to pre-reduce the PQ pool), and found no effects of 2 mM ATP ($p > 0.05$, Student's *t*-test). Possible effects of non-photochemical quenching were tested by measuring F_v/F_m values prior to- and after adenylate addition (see, for example, Fig. 6). F_v/F_m decreased by a small amount (about 5%) in the presence of 1 mM ATP (from 0.73 ± 0.02 to 0.69 ± 0.03, c.f. 0.71 ± 0.02 for the no adenylate control, n = 6–10 independent samples, mean ± S.D. reported), although no further decrease was observed on addition of additional ATP. It has been reported that ATP can induce state transitions in plant thylakoid preparations (from state 1 to state 2, quenching variable fluorescence [41]) when the thylakoid PQ pool is reduced, additional controls were undertaken. However, we found similar effects of ATP on PIFR in *A. thaliana* wild type and *stn7* mutant, deficient in state transitions [42] (SI Fig. S4).

The *in vitro* PIFR experiment is reliant upon the NADPH:Fd reductase activity of endogenous FNR to provide stromal reducing equivalents for NDH and FQR [11]. As such we tested the sensitivity of purified spinach FNR to ATP by means of an NADPH/Fd:cytochrome *c* reductase assay [28]. No effect on FNR activity was observed with 2 mM ATP ($p > 0.05$, Student's *t*-test). The remaining steps in CEF, *i.e.* turnover of the cytochrome b_6f complex and PSI, are common in LEF. We found no effects of ATP on the rate of *in vitro* LEF in uncoupled spinach thylakoid preparation as measured by light-dependent ferricyanide reduction ($p > 0.05$, Student's *t*-test), indicating that the ATP effect is likely specific to the PQ reductase. We note in passing that there is no evidence in the literature for the regulation of the respiratory homolog of NDH by adenylates, however the plastid enzyme exhibits considerable structural divergence from its respiratory counterpart [43,44].

To quantify the inhibition of PIFR we plotted the initial fluorescence rise kinetics (using a linear fit, see Materials and methods) as a function of adenylate (ATP or ADP) concentrations (Fig. 3). From four-parameter (sigmoidal) regression fits to these titration data we obtained IC_{50} (half-inhibitory concentration) values (± S.D.) for ATP inhibition of 0.98 ± 0.18 and 0.39 ± 0.04 mM for *A. hybridus* and spinach respectively, suggesting that the NDH- and FQR pathways of CEF (in their respective species) are inhibited by ATP, but that the latter is more sensitive. Both pathways were also inhibited by ADP, but at higher concentrations (IC50 values of 1.80 ± 0.40 and 1.23 ± 0.12 mM for *A. hybridus* and spinach respectively). Note also that while inhibition of

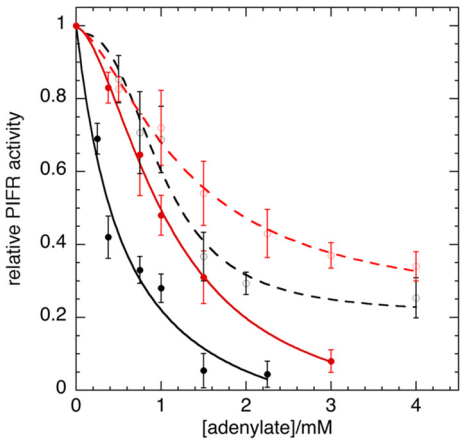

Fig. 3. *In vitro* PIFR activity as a function of adenylate (ATP (solid lines) and ADP (broken lines)) concentration in spinach (black) and *A. hybridus* (red) thylakoids. Initial rates of the PIFR were measured from fluorescence data normalised to F_{o*}. Ferredoxin was present at 1 µM, with other conditions as in Fig. 1. Data are presented from 4 to 5 independent replicates.

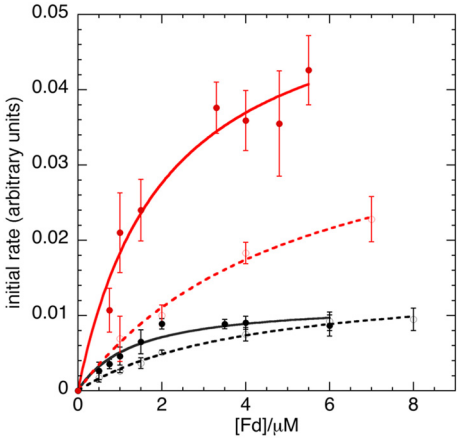

Fig. 4. Inhibition of the PIFR initial rise kinetics in *A. hybridus* (red) and spinach (black) in the presence of 0.75 mM- (spinach) and 1 mM (*A. hybridus*) ATP (dotted lines). Data from 4 to 6 independent experiments. Solid lines show the uninhibited rates as presented in Fig. 2.

both FQR and NDH activities by ATP appeared to be reasonably monotonic and was essentially complete at [ATP], above 3- and 2 mM, the inhibition by ADP appeared multiphasic and never reached completion at the highest concentrations, possibly indicating slightly different binding niches on the target enzyme (see below).

3.2. Competition between ATP and Fd at NDH and FQR

In our initial assays, we noticed that high concentrations of Fd could reverse inhibition of NDH inhibition by ATP. We thus performed a competition analysis of PIFR kinetics as a function of Fd concentration at fixed concentrations of ATP (Fig. 4). Using Cheng-Prusoff analysis [45] and assuming a competitive mode of inhibition of the initial rates of PIFR gives inhibitory (dissociation) constants (K_i, ± S.D.) of 240 (± 22)- and 670 (± 120) µM for the FQR- and NDH-related *in vitro* PIFR responses (in spinach and *A. hybridus*, respectively). Using the same approach, the K_i values for ADP inhibition of the PIFR in spinach (FQR) and *A. hybridus* (NDH) were found to be 0.7 (± 0.07) - and 1.2 (± 0.26) mM, respectively. For most enzyme-catalysed reactions it is reasonable to assume that K_m is approximately equal to the dissociation constant (K_d) for the enzyme-substrate (ES) complex (*i.e.* the ratio of the rate constants k_{off}/k_{on} for the formation of ES from free enzyme and substrate). Thus, we estimate that ATP binds 350-fold more weakly to NDH and 200-fold more weakly to FQR than substrate Fd under the *in vitro* conditions employed in the current study. Notably, ADP binds approximately 550-fold more weakly than Fd to both NDH and FQR, indicative of the differing selectivity for ATP over ADP in the enzyme systems under study.

3.3. Assessing ATP inhibition of NDH and FQR in a single species

While the *A. hybridus* and spinach systems are convenient for probing NDH and FQR inhibition, it is not clear from these experiments whether the observed differences in inhibition of NDH and FQR are related to species differences. We note, however, that NDH displays a high degree of sequence conservation in plants [11,43,46,47], likewise PGR5/PGRL1 [48]. Previously we have reported that about 75% of the PIFR in *A. thaliana* Col-0 *in vitro* is due to FQR activity and the remaining to NDH [11], thus making it possible to compare inhibition of the two pathways in a single species. Although difficulties in obtaining large quantities of chloroplasts exhibiting CEF activity from *A. thaliana* [27] prevented us from performing a detailed *in vitro* analysis, we were able to estimate a K_i value of 300 ± 100 µM (n = 3 independent replicates) for ATP inhibition of CEF (in the absence of AA) in this species.

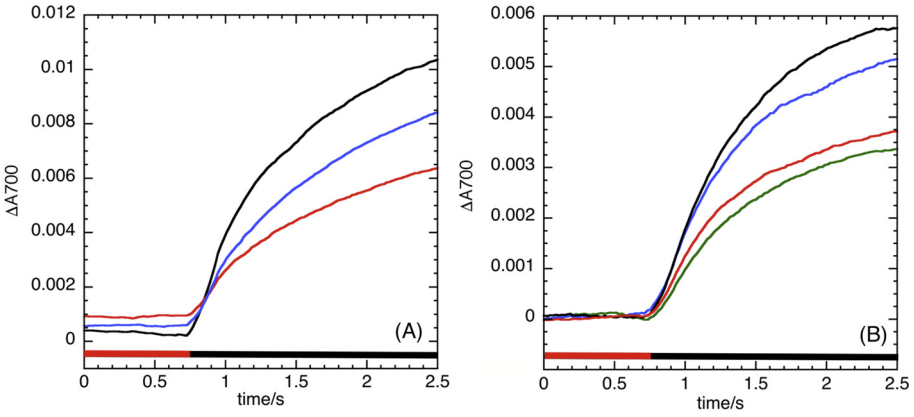

Fig. 5. Kinetics of CEF-mediated P700+ re-reduction in uncoupled broken *A. hybridus* (A) and spinach (B) chloroplast preparations as a function of ATP concentration, control (black trace), 1 mM ATP (blue trace), 2 mM ATP (red trace). The red- and black bars underneath the traces indicate the application- and removal of actinic light (620 nm, 250 μmol photons $m^{-2} s^{-1}$.), respectively. The green trace in panel (B) shows the effect of 10 μM AA on the rate of $P700^+$ re-reduction in spinach (10 μM AA was present in all measurements show in panel (A)). DCMU and hydroxylamine were present at 10 μM and 1 mM respectively to inhibit PSII activity. The sample also contained 1 μM Fd and 100 μM NADPH, acting as stromal electron donors. Representative data from 3 independent replicates. For further experimental details, refer to Materials and methods.

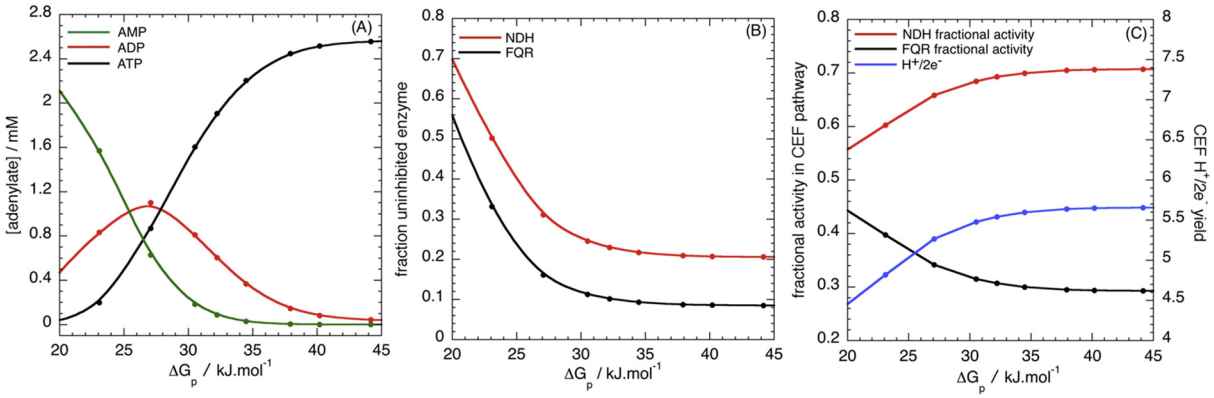

Fig. 6. (A) Predicted steady-state stromal adenylate (ATP (black), ADP (red), AMP (green)) concentrations as a function of phosphorylation potential. For the ODE simulation of the adenylate equilibria, initial conditions were 2 mM ADP, 4 mM phosphate, 0.6 mM AMP, and nil ATP, with a ΔG^o value for ATP hydrolysis of -30.5 kJ. mol^{-1}. The adenylate kinase equilibrium constant was set at 2.22 (in the direction of ADP formation). The simulation was run for 1000 (arbitrary) time points, by which point the concentrations of all components had reached a steady state. For further details, see Materials and methods. (B) Predicted fraction of uninhibited NDH (red) or FQR (black) as a function of phosphorylation potential. Note that both ADP- and ATP-inhibited forms of NDH and FQR were considered in the construction of this fig. (C) Fractional contributions to total (NDH + FQR) CEF of NDH (red) and FQR (black) and predicted net $H^+/2e^-$ yield (blue) of the CEF pathway as a function of phosphorylation potential (ΔG_p).

In the presence of AA the remaining PIFR activity in Col-0 broken chloroplast preparations also displayed sensitivity to ATP, with an estimated K_i value of 700 ± 100 μM, similar to that observed in *A. hybridus*. We thus conclude that, at least across the species we studied, FQR is about 2–3-fold more sensitive to ATP than NDH.

3.4. Measurement of $P700^+$ re-reduction kinetics validates the observation of inhibition of CEF by adenylates

As discussed above, the PIFR is a somewhat indirect assay for investigating CEF-related PQ reductase activity. An additional, more direct assay for CEF activity *in vitro* is provided by measuring absorbance changes associated with the redox status of P700 within PSI when electron donation from PSII is inhibited. Illumination of broken chloroplast preparations with red light in the presence of DCMU (blocking PSII activity) results in essentially full oxidation of P700 that, in the absence of electron donors, is only very slowly re-reduced in the dark. On addition of NADPH and Fd, the rate of re-reduction increases, reflecting activation of the CEF pathway(s) and reduction of the PQ pool (for details, see Materials and methods). Fig. 5A shows that the rate of $P700^+$ re-reduction in *A. hybridus* broken chloroplast preparations (in the presence of 10 μM AA) decreases progressively with increasing ATP, with a K_i of approximately 1 mM, consistent with results from the PIFR assay in the current study. In agreement with this observation, the rate of $P700^+$ re-reduction in broken chloroplast preparations from spinach (measured in the absence of AA) exhibits a similar sensitivity to ATP (Fig. 5B).

As a side note, the extent of re-reduction of $P700^+$ decreased with the addition of ATP, while the half time increased from approximately 350- to 550 ms in the presence of 2 mM ATP, most likely reflecting competition between PQ reduction by NDH and PQH_2 oxidation by the plastid terminal oxidase (PTOX), which becomes more pronounced when NDH is partially inhibited by ATP.

4. Discussion

The results above indicate that ATP inhibits both NDH and FQR pathways of CEF, at physiologically relevant concentrations, leading us to propose a straightforward model for regulation of CEF in plant chloroplasts in which CEF is activated under conditions when stromal ATP low, but is downregulated as ATP levels build up, allowing for effective ATP homeostasis. The differences in K_i values suggest a two-tiered regulatory system, where the highly efficient ($4H^+/2e^-$) proton pumping NDH is activated with moderate decreases in ATP, with the (presumably) less energetically efficient FQR pathway (which is unlikely to be thermodynamically constrained) being activated under more severe ATP depletion.

We develop this idea further using a first-order simulation the model the effects of stromal adenylate pool composition on NDH and FQR activity. Fig. 6A shows the expected stromal ATP, ADP and AMP steady -state concentrations as a function of a physiological range of phosphorylation potentials (ΔG_P), predicted using a simple 1st order

ordinary differential equation model using starting conditions for the composition of the adenylate and phosphate pool as reported in the literature [30,31,49] (for further details, see Materials and methods). These steady-state concentrations are consistent with those proposed on the basis of *pmf* measurement in spinach leaves [50]. Fig. 6B shows the predicted activities (fraction uninhibited) of NDH and FQR as a function of the adenylate pools calculated in Fig. 6A, assuming competitive inhibition with Fd at 1 μM. At $\Delta G_P > 30\,kJ\,mol^{-1}$, activity of FQR is predicted to be less than 10% its maximal activity, but increases sharply as ΔG_P decreases below about $27\,kJ\,mol^{-1}$. The activity dependence of NDH is similar with some complexities, with NDH activity predicted to increase sharply at $\Delta G_P < \sim 33\,kJ\,mol^{-1}$. However, the weaker K_i for ATP, in combination with the competitive nature of the inhibition with Fd, prevents full inhibition of NDH higher ΔG_P values, suggesting that this mode of regulation would leave NDH partially active under all conditions.

Fig. 6C shows the relative contributions of the two CEF pathways in a hypothetical (for illustrative purposes) chloroplast with equal V_{max} values for NDH and FQR. It should be noted that the model would need to be modified to account for actual enzyme content within the chloroplast, as well as other CEF regulators (see below). Nevertheless, the model provides a useful illustration of the effects of proposed adenylate regulation. NDH is predicted to contribute more under high ΔG_P conditions, whereas FQR constitutes progressively more as adenylate charge is decreased below about $30\,kJ\,mol^{-1}$. Because NDH-CEF involves the highly efficient proton pumping NDH complex, it should translocate $8H^+/2e^-$, whereas FQR is (presumably) not a proton pump and thus relies solely on the Q-cycle for proton pumping, resulting in $H^+/2e^-$ of 4 [10,11]. Using these values, the model predicts that, while the rate of CEF will increase with decreasing ΔG_P, the *efficiency* of proton translocation by CEF will decrease. Under moderate ATP deficits, the more efficient NDH pathway is preferred, but under severe deficits, the less thermodynamically constrained FQR pathway is activated. It may be that the more efficient NDH becomes thermodynamically limited at higher *pmf*, so that the build-up of larger extents of ΔpH needed to fully downregulate photosynthesis can only be produced using FQR.

The “ATP feedback mechanism” hypothesis that we propose here can, in a straightforward way, account for much of the known phenomenology of CEF and the regulation of the photosynthetic energy budget by activating the PQ reductases under ATP deficit, and is compatible with earlier proposals of regulation of CEF by ATP [12]. It should be noted that the current study does not answer whether any CEF occurs through the proposed cytochrome b_6f-PSI supercomplexes (although it is not incompatible with this suggestion), and does not exclude other proposed regulatory mechanisms for CEF [14,16,18,19,21]. Furthermore, additional studies are required to define the structural basis of the “ATP feedback mechanism” that we propose here. Nevertheless, the model can explain how a number of mutants that affect diverse metabolic processes, all produce a high CEF (*hcef*) phenotype. The majority of *hcef* mutants isolated in our past work showed defects in assimilatory, photorespiratory or related processes that likely induce futile cycling or require metabolic bypass pathways, both of which consume more ATP than the wild type metabolic pathways [13]. The resulting ATP deficit should activate NDH and/or FQR, tending to restore ATP/NADPH balance. We proposed in our earlier work that (tobacco) mutants with diminished glyceraldehyde-3-P-dehydrogenase (GAPDH) activity should accumulate bisphosphoglycerate, which is unstable and decays rapidly to phosphoglycerate, setting up a futile cycle that consumes ATP through the activity of phosphoglycerate kinase [51]. More recently, it has been suggested that *hcef1*, which is defective in chloroplast fructose-1,6-bisphosphotase (FBPase), bypasses the *hcef1* lesion through an alternative assimilatory “shunt” that uses the cytosolic FBPase [52]. The new pathway is metabolically balanced for NADPH but uses three extra ATPs (one at phosphoribulokinase and two at PGA kinase), potentially inducing a strong ATP deficit that could lead to activation of NDH-CEF by releasing inhibition of NDH.

Another common phenotype of *hcef* mutants is increased production of H_2O_2, and we have demonstrated that induction of H_2O_2 by itself can induce high rates of CEF [53]. We hypothesized that high levels of H_2O_2 could either active CEF directly (by increasing NDH expression and enzyme activity, or indirectly, inducing ATP deficits. The data presented here suggest that the latter model is the most parsimonious, because any imbalance in ATP consumption would results in elevated CEF, and there are several plausible mechanisms by which H_2O_2 could elevate ATP demand, *e.g.* altering the thiol redox regulation (governed by the ferredoxin/thioredoxin (Fd/TRX) system) that normally acts to prevent futile cycling between the light and dark adapted states of CBB cycle- or oxidative pentose phosphate pathway enzymes. Excess H_2O_2 can effectively oxidize free thiol groups, either directly or possibly through the peroxiredoxin system, or induce post-translational modifications such protein nitrosylation or glutathionylation, potentially resulting in regulatory states where both anabolic and catabolic enzymes are simultaneously active, inducing futile cycling that would deplete ATP and thus activate CEF [54].

It is important to note, that there is independent evidence for additional regulation of CEF in plant chloroplasts, that can provide further tuning mechanisms for both pathways, such as, TROL activity, thiol status, phosphorylation, redox poise and membrane heterogeneity [10,14,24,27,54,55]. However, our results suggest that the proposed ATP feedback mechanism may well be the most rapidly responding. The effects of ATP addition were rapidly induced, as is seen in *e.g.* Fig. 2A and B where the PIFR measured a few seconds after ATP addition was strongly inhibited, implying that the on rate for inhibition is very rapid. Because the inhibition is reversible (*e.g.* addition of Fd decreased inhibition) and has a relatively high K_i, we conclude that the off rate for ATP under physiological conditions is similarly fast. Thus, ATP feedback may account for critical energy balancing under fluctuating environmental conditions, especially light intensities, which are known to strongly impact mutants defective in CEF or the buildup of ΔpH [5,56].

In conclusion, the data presented here lead to a straightforward mechanism for the management of the plastid energy budget in vascular plants *via* adenylate regulation of CEF activity, that may be particularly important under rapid fluctuations in the ATP/NADPH energy budget.

Author contributions

Author contributions: N.F. and D.M.K. conceived the study and designed experiments; D.M.K. constructed equipment; N.F. performed experiments; N.F., D.M.K. and T.M.B. analyzed data; N.F., T.M.B. and D.M.K. contributed to the preparation of the manuscript.

Transparency document

The Transparency document associated with this article can be found, in online version.

Acknowledgments

We thank Vanessa Quevedo and Kailey Miller for assistance with the growth- and care of *A. hybridus*. This work was supported by grants DE-FG02-91ER20021 and DE-FG02-09ER20310 from the Photosynthetic Systems program from Division of Chemical Sciences, Geosciences, and Biosciences, Office of Basic Energy Sciences of the U.S. Department of Energy (to D.M.K. and T.M.B. respectively). In addition, a portion of D.M.K.'s salary is supported by MSU AgBioResearch.

Appendix A. Supplementary data

Supplementary data to this article can be found online at https://

doi.org/10.1016/j.bbabio.2019.148081.

References

[1] J.A. Cruz, et al., Plasticity in light reactions of photosynthesis for energy production and photoprotection, J. Exp. Bot. 56 (2005) 395–406.

[2] X.-P. Li, P. Muller-Moule, A.M. Gilmore, K.K. Niyogi, PsbS-dependent enhancement of feedback de-excitation protects photosystem II from photoinhibition, Proc. Natl. Acad. Sci. U. S. A. 99 (2002) 15222–15227.

[3] M.D. Brooks, S. Jansson, K.K. Niyogi, PsbS-dependent non-photochemical quenching, Adv Photosynth Resp 40 (2014) 297–314.

[4] D.M. Kramer, J.A. Cruz, A. Kanazawa, Balancing the central roles of the thylakoid proton gradient, Trends Plant Sci. 8 (2003) 27–32.

[5] A. Kanazawa, et al., Chloroplast ATP synthase modulation of the thylakoid proton motive force: implications for photosystem I and photosystem II photoprotection, Front. Plant Sci. 8 (2427–2412) (2017).

[6] U. Armbruster, et al., Regulation and levels of the thylakoid K^+/H^+ antiporter KEA3 shape the dynamic response of photosynthesis in fluctuating light, Plant Cell Physiol 57 (2016) 1557–1567.

[7] J. Kromdijk, et al., Improving photosynthesis and crop productivity by accelerating recovery from photoprotection, Science 354 (2016) 857–861.

[8] J.F. Allen, Cyclic, pseudocyclic and noncyclic photophosphorylation: new links in the chain, Trends Plant Sci. 8 (2003) 15–19.

[9] T. Shikanai, Regulatory network of proton motive force: contribution of cyclic electron transport around photosystem I, Photosynth. Res. 129 (2016) 253–260.

[10] D.D. Strand, N. Fisher, D.M. Kramer, H. Kirchhoff (Ed.), Chloroplasts: Current Research and Future Trends, Caister Academic Press, Poole, UK, 2016, pp. 89–100.

[11] D.D. Strand, N. Fisher, D.M. Kramer, The higher plant plastid NAD(P)H dehydrogenase-like complex (NDH) is a high efficiency proton pump that increases ATP production by cyclic electron flow, J. Biol. Chem. 292 (2017) 11850–11860.

[12] P. Joliot, A. Joliot, Cyclic electron transfer in plant leaf, Proc. Natl. Acad. Sci. U. S. A. 99 (2002) 10209–10214.

[13] A.K. Livingston, J.A. Cruz, K. Kohzuma, A. Dhingra, D.M. Kramer, An Arabidopsis mutant with high cyclic electron flow around photosystem I (*hcef*) involving the NDH complex, Plant Cell 22 (2010) 221–233.

[14] J. Alric, J. Lavergne, F. Rappaport, Redox and ATP control of photosynthetic cyclic electron flow in *Chlamydomonas reinhardtii* (I) aerobic conditions, Biochim. Biophys. Acta 1797 (2010) 44–51.

[15] A. Takabayashi, M. Kishine, K. Asada, T. Endo, F. Sato, Differential use of two cyclic electron flows around photosystem I for driving CO_2-concentration mechanism in C4 photosynthesis, Proc Natl Acad Sci USA 102 (2005) 16898–16903.

[16] F. Chaux, G. Peltier, X. Johnson, A security network in PSI photoprotection: regulation of photosynthetic control, NPQ and O_2 photoreduction by cyclic electron flow, Front. Plant Sci. 6 (875) (2015).

[17] D. D. Strand, D. M. Kramer, in Adv Photosynth Resp, B. Demmig-Adams, G. Garab, W. Adams III, Govindjee, Eds. (Springer, The Netherlands, 2014), vol. XXXVIII, pp. 387–408.

[18] G. Finazzi, et al., Involvement of state transitions in the switch between linear and cyclic electron flow in Chlamydomonas reinhardtii, EMBO Rep. 3 (2002) 280–285.

[19] H. Takahashi, S. Clowez, F.A. Wollman, O. Vallon, F. Rappaport, Cyclic electron flow is redox-controlled but independent of state transition, Nat. Commun. 4 (1954) (2013), https://doi.org/10.1038/ncomms2954.

[20] B. Lucker, D.M. Kramer, Regulation of cyclic electron flow in *Chlamydomonas reinhardtii* under fluctuating carbon availability, Photosynth. Res. 117 (2013) 449–459.

[21] M. Terashima, et al., Calcium-dependent regulation of cyclic photosynthetic electron transfer by a CAS, ANR1, and PGRL1 complex, Proc. Natl. Acad. Sci. U. S. A. 109 (2012) 17717–17722.

[22] H. Xue, S.V. Bergner, M. Scholz, M. Hippler, Novel insights into the function of LHCSR3 in *Chlamydomonas reinhardtii*, Plant Signal. Behav. 10 (2015) e1058462.

[23] A.K. Hochmal, S. Schulze, K. Trompelt, M. Hippler, Calcium-dependent regulation of photosynthesis, Biochim. Biophys. Acta 1847 (2015) 993–1003.

[24] L. Michelet, et al., Redox regulation of the Calvin-Benson cycle: something old, something new, Front. Plant Sci. 4 (470) (2013).

[25] A.K. Hochmal, et al., Calredoxin represents a novel type of calcium-dependent sensor-responder connected to redox regulation in the chloroplast, Nat Comms 7 (2016) 1–14, https://doi.org/10.1038/ncomms11847.

[26] D.D. Strand, et al., Activation of cyclic electron flow by hydrogen peroxide in vivo, Proc. Natl. Acad. Sci. U. S. A. 112 (2015) 5539–5544.

[27] D.D. Strand, N. Fisher, G.A. Davis, D.M. Kramer, Redox regulation of the antimycin A sensitive pathway of cyclic electron flow around photosystem I in higher plant thylakoids, Biochim. Biophys. Acta 1857 (2016) 1–6.

[28] N. Fisher, D.M. Kramer, Non-photochemical reduction of thylakoid photosynthetic redox carriers in vitro: relevance to cyclic electron flow around photosystem I? Biochim. Biophys. Acta 1837 (2014) 1944–1954.

[29] C. C. Hall, Cruz, J., Wood, M., Zegerac, R., De Mars, D., Carpenter, J. F., Kanazawa, A., and Kramer, D. M., in Photosynthesis Research for Food, Fuel and Future, T. Kuang, Lu, C., and Zhang, L., Ed. (Springer, Heidelberg, Germany, 2013), pp. 184–188.

[30] M. Stitt, R.M. Lilley, H.W. Heldt, Adenine nucleotide levels in the cytosol, chloroplasts, and mitochondria of wheat leaf protoplasts, Plant Physiol. 70 (1982) 971–977.

[31] H. Usuda, Adenine nucleotide levels, the redox state of the NADP system, and assimilatory force in nonaqueously purified mesophyll chloroplasts from maize leaves under different light intensities, Plant Physiol. 88 (1988) 1461–1468.

[32] J. Rosing, E.C. Slater, The value of ΔG° for the hydrolysis of ATP, Biochim. Biophys. Acta 267 (1972) 275–290.

[33] T. Shikanai, et al., Directed disruption of the tobacco ndhB gene impairs cyclic electron flow around photosystem I, Proc. Natl. Acad. Sci. U. S. A. 95 (1998) 9705–9709.

[34] P.A. Burrows, L.A. Sazanov, Z. Svab, P. Maliga, P.J. Nixon, Identification of a functional respiratory complex in chloroplasts through analysis of tobacco mutants containing disrupted plastid ndh genes, EMBO J. 17 (1998) 868–876.

[35] Y. Okegawa, Y. Kagawa, Y. Kobayashi, T. Shikanai, Characterization of factors affecting the activity of photosystem I cyclic electron transport in chloroplasts, Plant Cell Physiol 49 (2008) 825–834.

[36] A. Takabayashi, T. Endo, T. Shikanai, F. Sato, Post-illumination reduction of the plastoquinone pool in chloroplast transformants in which chloroplastic NAD(P)H dehydrogenase was inactivated, Biosci. Biotechnol. Biochem. 66 (2002) 2107–2111.

[37] T. Endo, T. Shikanai, F. Sato, K. Asada, NAD(P)H dehydrogenase-dependent, antimycin A-sensitive electron donation to plastoquinone in tobacco chloroplasts, Plant Cell Physiol 39 (1998) 1226–1231.

[38] A. Jajoo, S. Bharti, P. Mohanty, Evaluation of the specific roles of anions in electron transport and energy transfer reactions in photosynthesis, Photosynthetica 39 (2001) 321–337.

[39] P. Horton, M.T. Black, Light-dependent quenching of chlorophyll fluorescence in pea chloroplasts induced by adenosine 5′-triphosphate, Biochim. Biophys. Acta 635 (1981) 53–62.

[40] U. Schreiber, ATP-induced increase in chlorophyll fluorescence. Characterization of rapid and slow induction phases, Biochim. Biophys. Acta 767 (1984) 70–79.

[41] W.S. Chow, A. Telfer, D.J. Chapman, J. Barber, State 1-state 2 transition in leaves and its association with ATP-induced chlorophyll fluorescence quenching, Biochim. Biophys. Acta 638 (1981) 60–68.

[42] S. Bellafiore, F. Barneche, G. Peltier, J.-D. Rochaix, State transitions and light adaptation require chloroplast thylakoid protein kinase STN7, Nature 433 (2005) 892–895.

[43] M. Suorsa, S. Sirpiö, E.-M. Aro, Towards characterization of the chloroplast NAD(P)H dehydrogenase complex, Mol. Plant 2 (2009) 1127–1140.

[44] T.G. Laughlin, A.N. Bayne, J.-F. Trempe, D.F. Savage, K.M. Davies, Structure of the complex I-like molecule NDH of oxygenic photosynthesis, Nature 566 (2019) 411–414.

[45] Y. Cheng, W.H. Prusoff, Relationship between the inhibition constant (K_i) and the concentration of inhibitor which causes 50 per cent inhibition (I50) of an enzymatic reaction, Biochem. Pharmacol. 22 (1973) 3099–3108.

[46] Y. Munekage, et al., PGR5 is involved in cyclic electron flow around photosystem I and is essential for photoprotection in Arabidopsis, Cell 110 (2002) 361–371.

[47] K. Ifuku, T. Endo, T. Shikanai, E.-M. Aro, Structure of the chloroplast NADH dehydrogenase-like complex: nomenclature for nuclear-encoded subunits, Plant Cell Physiol 52 (2011) 1560–1568.

[48] G. DalCorso, et al., A complex containing PGRL1 and PGR5 is involved in the switch between linear and cyclic electron flow in *Arabidopsis*, Cell 132 (2008) 273–285.

[49] T.D. Sharkey, P.J. Vanderveer, Stromal phosphate concentration is low during feedback limited photosynthesis, Plant Physiol. 91 (1989) 679–684.

[50] P. Joliot, A. Joliot, Quantification of the electrochemical proton gradient and activation of ATP synthase in leaves, Biochim. Biophys. Acta 1777 (2008) 676–683.

[51] A.K. Livingston, A. Kanazawa, J.A. Cruz, D.M. Kramer, Regulation of cyclic electron transfer in C3 plants: differential effects of limiting photosynthesis at rubisco and glyceraldehyde-3-phosphate dehydrogenase, Plant Cell Environ. 33 (2010) 1779–1788.

[52] T.D. Sharkey, S.E. Weise, The glucose 6-phosphate shunt around the Calvin-Benson cycle, J. Exp. Bot. 67 (2015) 4067–4077.

[53] D.D. Strand, et al., Defects in the expression of chloroplast proteins leads to H_2O_2 accumulation and activation of cyclic electron flow around photosystem I, Front. Plant Sci. 7 (825–816) (2017).

[54] M. Muthuramalingam, A. Matros, R. Scheibe, H.P. Mock, K.J. Dietz, The hydrogen peroxide-sensitive proteome of the chloroplast in vitro and in vivo, Front. Plant Sci. 4 (54) (2013).

[55] L. Vojta, et al., TROL-FNR interaction reveals alternative pathways of electron partitioning in photosynthesis, Sci. Rep. 5 (2015) 10085, , https://doi.org/10.1038/srep10085.

[56] M. Suorsa, et al., PROTON GRADIENT REGULATION5 is essential for proper acclimation of Arabidopsis photosystem I to naturally and artificially fluctuating light conditions, Plant Cell 24 (2012) 2934–2948.